NIH Public Access
Author Manuscript
Pulm Pharmacol Ther. Author manuscript; available in PMC 2014 April 01.

Published in final edited form as:
Pulm Pharmacol Ther. 2013 April ; 26(2): 296–304. doi:10.1016/j.pupt.2012.12.009.

NOVEL LOW MOLECULAR WEIGHT LIGNINS AS POTENTIAL ANTIEMPHYSEMA AGENTS: IN VITRO TRIPLE INHIBITORY ACTIVITY AGAINST ELASTASE, OXIDATION AND INFLAMMATION

Bhawana Saluja[1], **Jay N. Thakkar**[2], **Hua Li**[1], **Umesh R. Desai**[2], and **Masahiro Sakagami**[1,*]

Bhawana Saluja: Bhawana.Saluja@fda.hhs.gov; Jay N. Thakkar: thakkarj@gmail.com; Hua Li: lihua@vcu.edu; Umesh R. Desai: urdesai@vcu.edu; Masahiro Sakagami: msakagam@vcu.edu

[1]Department of Pharmaceutics, School of Pharmacy, Virginia Commonwealth University, 410 N. 12th Street, P. O. Box 980533, Richmond, Virginia 23298, USA

[2]Department of Medicinal Chemistry and Institute for Structural Biology and Drug Discovery, Virginia Commonwealth University, 800 East Leigh Street, Richmond, Virginia 23219, USA

Abstract

No molecule has been found to be effective against emphysema to date primarily because of its complex pathogenesis that involves elastolysis, oxidation and inflammation. We here describe novel unsulfated or sulfated low molecular weight lignins (LMWLs) chemo-enzymatically prepared from 4-hydroxycinnamic acids monomers, as the first potent triple-action inhibitors of neutrophil elastase, oxidation and inflammation. The inhibitory potencies of three different cinnamic acid-based LMWLs were determined in vitro using chromogenic substrate hydrolysis assays, radical scavenging and lung cellular oxidative biomarker reduced glutathione (rGSH) assays, and lung cellular inflammatory biomarker NFκB and IL-8 assays, respectively. Each LWML uniquely displayed triple-action inhibition, among which CDSO3, a sulfated caffeic acid-based LMWL, was most potent. The half-maximal anti-human neutrophil elastase (HNE) potency of CDSO3 was 0.43 μM. This high potency arose from lignin-like oligomerization, which was further potentiated by 6.6-fold due to sulfation. Mechanistically, this elastase inhibition was of mixed-type, time-dependent and more selective to positively charged elastases. The half-maximal anti-oxidative potency of CDSO3 was 3.52 μM, 4.8-fold potentiated from that of the monomer, caffeic acid (CA). In contrast, the half-maximal inhibitory potency to TNFα-induced inflammation was 5–10 μM, despite no activity with the monomer. More intriguingly, this anti-inflammatory activity was essentially identical with different stimuli, okadaic acid and hydrogen peroxide (H_2O_2), which implied that CDSO3 acts directly on inflammatory cascades within the cells. Overall, oligomerization and sulfation produced or significantly potentiated the activity, in comparison to the monomer. Thus, sulfated and unsulfated LMWLs are novel non-peptidic 2.8–4.1 kDa macromolecules that exhibit for the first time potent triple inhibitory activity against elastase, oxidation and inflammation, the three major pathogenic mechanisms known to cause emphysema.

© 2012 Elsevier Ltd. All rights reserved.

*Please send all correspondence to: Masahiro Sakagami, Ph.D., Department of Pharmaceutics, School of Pharmacy, Virginia Commonwealth University, 410 N 12th Street, P.O. Box 980533, Richmond, VA 23298-0533, USA, Phone: +1-(804)828-2014, Fax: +1-(804)828-8359, msakagam@vcu.edu.

Publisher's Disclaimer: This is a PDF file of an unedited manuscript that has been accepted for publication. As a service to our customers we are providing this early version of the manuscript. The manuscript will undergo copyediting, typesetting, and review of the resulting proof before it is published in its final citable form. Please note that during the production process errors may be discovered which could affect the content, and all legal disclaimers that apply to the journal pertain.

NIH-PA Author Manuscript
NIH-PA Author Manuscript
NIH-PA Author Manuscript

NIH-PA Author Manuscript

NIH-PA Author Manuscript

NIH-PA Author Manuscript

Keywords

Emphysema; Elastase; Inflammation; Oxidation; Caffeic acid; Oligomer

1. INTRODUCTION

Emphysema is one of the major pathological manifestations of COPD, chronic obstructive pulmonary disease, which causes high and still-increasing morbidity and mortality in the United States and worldwide [1]. Closely associated with chronic cigarette smoking, this disease develops moderate-to-severe shortness of breath (dyspnea), resulting in physical and functional disability and eventually death, due to the progressive destruction and loss of the alveolar septa and the abnormal airspace enlargement in the lung [2,3]. At present, however, the treatment of emphysema and COPD is still limited and only marginally successful [4–6]. No drug has been shown to prevent or cure the disease or reduce its progression. In fact, drugs presently used in managing emphysema and COPD, bronchodilators and inhaled corticosteroids, simply reduce frequency and severity of exacerbations [4–6]. Therefore, there has been a pressing need to discover and develop novel drug entities that enable effective prevention and/or treatment of emphysema and COPD [4–6].

The lack of effective therapy to prevent and/or treat emphysema is largely due to its multi-faced pathogenic complexity that remains not fully understood even today [3,6–8]. Induced elastolysis, oxidative stress and inflammation in different lung cells have been long suggested as three major pathogenic mechanisms causing emphysema [3,7,8]. However, nearly all single-mechanism inhibitors developed for this multi-faced pathogenic disease have failed to reach clinical applications, although their benefits were demonstrated in cells and animals. This was partly because most of these preclinical studies were centered on testing inhibitors in the disease states induced with mechanistically corresponding agents. For example, elastase inhibitors were shown to be effective in elastase-induced emphysema models, but rarely tested in oxidation- or inflammation-induced models [3,7–9]. Likewise, antioxidants have been primarily tested in oxidation- or inflammation-induced emphysema models, but rarely in elastase-induced models [3,7–9]. The consistent failures with these single-mechanism inhibitors should thus raise a critical question whether dual or triple inhibitory actions would be better to treat multi-faced complex pathogenesis of emphysema. In support of this argument, molecules exerting dual inhibitory activities, e.g., anti-oxidative and anti-inflammatory, as exemplified by curcumin and resveratrol, have demonstrated better control on the triple-threat pathogenesis [10–12]. Similarly, new dual-acting coumarinic derivatives have been discovered to be anti-oxidative and anti-elastase, which thereby moderately inhibit the subsequent cascade of elastase-induced inflammation [13]. However, no molecule has been discovered to date that exhibit triple-action inhibition of anti-elastase, anti-oxidation and anti-inflammation.

We have recently synthesized and discovered low molecular weight lignins (LMWLs) based on 4-hydroxycinnamic acids scaffold (Figure 1) as novel potent dual-action inhibitors of blood serine proteases, factor Xa and thrombin [14–16]. While these serine protease activities appeared to arise from the unique lignin-like oligomeric scaffolds with or without sulfation [14–16], the monomers from which these LMWLs were prepared, i.e., 4-hydroxycinnamic acids, are phenolic molecules, which have been shown to be antioxidants by virtue of their radical scavenging and trapping activity [17,18]. Moreover, as structural relatives of flavonoids, certain derivatives of 4-hydroxycinnamic acids have been shown to be anti-inflammatory, inhibiting activation of the inflammatory transcription factor, nuclear factor kappa B (NFκB) [19,20]. Hence, we hypothesized that the anti-oxidative and anti-inflammatory activities of the monomers will be maintained or enhanced upon the

NIH-PA Author Manuscript

NIH-PA Author Manuscript

NIH-PA Author Manuscript

oligomerization, together with anti-serine protease activity of cinnamic acid-based LMWLs, such that LMWLs (Figure 1) would possess for the first time the triple inhibitory activity to elastase, oxidation and inflammation. Accordingly, this study tested and characterized unsulfated or sulfated LMWLs of three 4-hydroxycinnamic acids, caffeic acid (CD and CDSO3), ferulic acid (FDSO3) and sinapic acid (SDSO3), with respect to the in vitro triple inhibitory activity against neutrophil elastase, oxidation and inflammation for projected therapeutic use in emphysema and COPD.

2. MATERIALS AND METHODS

2.1. Low molecular weight lignins (LMWLs), reference molecules and reagents

Unsulfated or sulfated LMWLs of three 4-hydroxycinnamic acids, CD, CDSO3, FDSO3 and SDSO3, shown in Figure 1, were synthesized chemo-enzymatically from caffeic acid, ferulic acid or sinapic acid, as described previously [14–16] and stored as 5 mM phosphate-buffered saline solutions at −20 °C prior to use. They had been characterized with respect to the range of oligomer chain length, sulfate groups per monomer unit and weight-average molecular weight, as described in Figure 1 [15]. As reference molecules, caffeic acid (CA) and fluticasone propionate (FP) were purchased from Sigma-Aldrich (St. Louis, MO), and Trolox® (6-hydroxyl-2,5,7,8-tertamethylchroman-2-carboxylic acid) was from Cayman Chemical Co. (Ann Arbor, MI). Unless otherwise indicated, all reagents were obtained from Sigma-Aldrich.

2.2. Lung epithelial cell culture: A549 and Calu-3 cells

Human alveolar A549 and bronchial Calu-3 epithelial cells received from the American Type Culture Collection (ATCC; Rockville, MD) were propagated and maintained in culture, in accordance with the ATCC-published protocols. The culture media were F-12K medium (ATCC) and Eagle's minimum essential medium (EMEM; ATCC), respectively, supplemented with 10 % fetal bovine serum (FBS; Invitrogen, Carlsbad, CA) and 1 % penicillin-streptomycin (10,000 U/ml and 10 mg/ml). These cells were cultured in the incubator (NAPCO, Millville, NJ) at 37 °C under the humidified 95 % air and 5 % CO_2. The cells were passaged every 4 and 6 days, respectively, upon trypsin-ethylenediaminetetraacetic acid (Trypsin-EDTA) treatment.

2.3. In vitro anti-elastase activity assessment: chromogenic substrate hydrolysis assay

The anti-elastase activities of LMWLs and CA were first determined via human neutrophil elastase (HNE) hydrolysis of a chromogenic substrate, *N*-methoxysuccinyl Ala-Ala-Pro-Val *p*-nitroanilide (MeOSuc-AAPV-*p*NA) at 37° C in a 96-well plate format. As stock solutions, HNE (salt-free, lyophilized; Athens Research and Technology, Inc., Athens, GA) was reconstituted at 8.0 U/ml in 50 mM acetate buffer (pH 5.5), whereas MeOSuc-AAPV-*p*NA was prepared at 8.7 mM in dimethyl sulfoxide (DMSO). The hydrolysis of 0.2 mM substrate by 24.2 mU/ml HNE was determined in 0.1 M sodium phosphate buffer (pH 7.6) and 0.25 M sodium chloride (NaCl) in the absence or presence of LMWLs or CA via absorbance increase at 405 nm (ΔAbs_{405}; in proportion to *p*NA generation) using the Synergy™2 microplate reader (BioTek Instruments, Inc., Winooski, VT). In parallel, the absorbance was also monitored for LMWLs or CA without HNE to correct for their inherent absorbance, i.e., to be subtracted from the observed absorbance at each time. The initial linear hydrolysis rate (Y) represented by the absorbance increase in the first 10 min ($\Delta Abs_{405,10min}$) was plotted as a function of logarithmic concentration (C) of LMWLs and CA. The half-maximal (50 %) inhibitory concentration (IC_{50}) and Hill slope (HS) values were then determined via curve-fitting to the 4-parameter logistic function equation:

NIH-PA Author Manuscript

NIH-PA Author Manuscript

NIH-PA Author Manuscript

$$Y=Y_{min}+(Y_0-Y_{min})/[1+(C/IC_{50})^{HS}]$$

where Y_0 is $\Delta Abs_{405,10min}$ in the absence of the test molecules; Y_{min} is the lowest asymptotic $\Delta Abs_{405,10min}$ seen at the highest concentration (e.g., 100 μM). The nonlinear regression curve-fitting employed Scientist® (MicroMath, St Louis, MO), in which the IC_{50} and HS values were floated for determination, while the Y_0 and Y_{min} values were fixed as obtained experimentally. The "goodness-of-fit" of the curve-fitting was assessed using the Scientist®-deriving statistical values for the coefficient of determination and model selection criterion; these were satisfactorily high at ≥0.993 and ≥4.0, respectively.

CDSO3 was then tested with respect to its inhibition kinetics, time-dependence and elastase specificity. The hydrolysis rates of varying 0.02–0.40 mM substrate by a fixed 24.2 mU/ml HNE were determined in the absence or presence of 1.0 μM CDSO3. The Eadie-Hofstee plots were used to deduce the inhibition kinetics from the derived apparent K_m and V_{max} values (the Michaelis constant and maximum rate, respectively). The HNE hydrolysis was also assessed following 0–90 min preincubation of 24.2 mU/ml HNE and 0.3, 0.7 or 1.0 μM CDSO3. The fractional remaining HNE activities were then determined, compared to those for the corresponding controls (i.e., in the absence of CDSO3). Finally, CDSO3 was tested in the hydrolysis of 0.2 mM MeOSuc-AAPV-*p*NA by 3.8 mU/ml human sputum elastase (HSE; 875 U/mg; Elastin Products Co., Inc., Owensville, MO) and 350 mU/ml porcine pancreatic elastase (PPE; 82 U/mg; Elastin Products Co., Inc.) under the same protocol; the IC_{50} and HS values were similarly determined.

2.4. In vitro anti-elastase activity assessment: functional insoluble elastin degradation assay

The functional inhibitory activity of CDSO3 on the hydrolysis of insoluble elastin by HSE was determined spectrophotometrically using elastin-congo red as a substrate, according to the method by Fujie et al [21]. Briefly, elastin-congo red ground with a motor and a pestle into uniform-size particles was suspended in 0.1 M Tris-HCl buffer (pH 8.0) and 0.2 M NaCl. HSE at 3.5 mU/ml (4 μg/ml) was incubated for 1 h at 37 °C with 2 mg/ml elastin-congo red suspension in the absence or presence of 0.1–0.5 μM CDSO3 in a total volume of 0.5 ml. The elastolytic reaction was then terminated by adding 0.5 ml of 0.1 M acetic acid, followed by centrifugation at 13,350 *g* for 10 min (Eppendorf, Westbury, NY). The absorbance of the supernatant was measured at 495 nm using the spectrophotometer (Shimadzu Corporation, Kyoto, Japan). In parallel, the absorbance was also determined for elastin-congo red and CDSO3 without HSE to correct for their inherent absorbance.

2.5. In vitro anti-oxidative activity assessment: chemical anti-oxidation assay

The anti-oxidative activities of LMWLs and CA were first determined using the chemical antioxidant assay kit (Cayman Chemical Co.) in a 96-well plate format, in accordance with the manufacturer's protocol. The assay employed formation of a chromogenic radical cation $ABTS^{\bullet+}$ from ABTS, 2,2′-azinobis(3-ethyl-benzothiazoline-6-sulphonic acid), by hydrogen peroxide (H_2O_2) in the presence of metmyoglobin at room temperature. This was monitored as absorbance increase at 750 nm (ΔAbs_{750}) using the microplate reader. A water soluble tocopherol analogue, Trolox® was used as a reference antioxidant and assessed under the same protocol. The initial rate of $ABTS^{\bullet+}$ production (Y) was assessed with the linear absorbance increase in the first 5 min ($\Delta Abs_{750,5min}$) and plotted as a function of logarithmic concentration (C) of LMWLs, CA or Trolox®. The IC_{50} and HS values were then determined via the nonlinear regression curve-fitting (Scientist®) to the equation used above. The "goodness-of-fit" parameters of the curve-fitting, the coefficient of

NIH-PA Author Manuscript

NIH-PA Author Manuscript

NIH-PA Author Manuscript

determination and model selection criterion values were satisfactorily high at ≥0.992 and ≥3.5, respectively.

2.6. In vitro anti-oxidative activity assessment: H_2O_2-induced rGSH assay in A549 cells

The cellular anti-oxidative activity was assessed for CDSO3 in the A549 cells stimulated with H_2O_2 using reduced glutathione (rGSH) as an oxidative stress marker. In 6-well plates, the A549 cells seeded at 0.4×10^6 cells/well were grown to 80–90 % confluence in culture for 72–96 h in 2.5 ml media. The cells were then incubated for 3 h in the F-12K media with 1 % FBS in the absence or presence of 0.1 mM H_2O_2 and/or 1 or 10 μM CDSO3. The cellular levels of total GSH (tGSH) and glutathione disulfide (GSSG, the oxidized form) were determined by the enzymatic recycling method developed by Rahman et al [22] with slight modifications. Briefly, the cells were counted and then lysed in 1.0 ml of 0.1 M potassium phosphate buffer (pH 7.5) with 5 mM EDTA, 0.1 % Triton-X and 0.6 % sulfosalicylic acid. The cell lysate supernatants (0.02 ml) were incubated for 30 s with 0.28 mg/ml 5,5′-dithiobis-(2-nitrobenzoic acid) (DTNB) and 1.41 U/ml glutathione reductase (GR) in a total volume of 0.14 ml. Following addition of 0.2 mg/ml β-nicotinamide adenine dinucleotide phosphate (βNADPH; 0.06 ml), the DTNB-GSH reaction was monitored as absorbance increase at 412 nm with the microplate reader for tGSH determination. For GSSG determination, the cell lysate supernatants (0.1 ml) were first incubated with 2-vinyl pyridine (2-VP; 0.002 ml) for 1 h at room temperature, followed by neutralization of excess 2-VP with triethanolamine (0.006 ml). The DTNB reaction with GSH originated from GSSG was then monitored at 412 nm following additions of DTNB, GR and βNADPH, similar to the tGSH determination described above. The cellular tGSH and GSSG levels were both normalized by the cell count and expressed as nmoles/10^6 cells. Finally, the cellular rGSH levels were calculated from:

$$\mathrm{rGSH} = \mathrm{tGSH} - 2 \times \mathrm{GSSG}$$

2.7. In vitro anti-inflammatory activity assessment: NFκ B and IL-8 assays in Calu-3 cells

The cellular anti-inflammatory activities of LMWLs and CA alongside FP were assessed in the Calu-3 cells stimulated with tumor necrosis factor α (TNFα) using nuclear factor kappa B (NFκB) and interleukin 8 (IL-8) as inflammatory transcription factor and chemokine, respectively. The Calu-3 cells (passage 19) plated at 0.5×10^6 cells/well in 12-well plates were cultured for 24 h. For NFκB assessments, the cells were transfected with custom-made plasmid NFκB tagged with luciferase enzyme gene (pNFκB-Luc; VCU Molecular Biology Core Facility, Richmond, VA) using the Effectene® transfection kit (Buffer EC, Enhancer and Effectene; QIAGEN, Inc., Valencia, CA) under the protocol slightly modified in-house. Briefly, the master-mix transfection solution was prepared by 10 min incubation of 0.6 μg pNFκB-Luc in 0.075 ml Buffer EC and 0.005 ml Enhancer, followed by 10 min incubation with 0.005 ml Effectene. This master-mix solution was diluted to 1 ml with the culture media and added to each well for 24 h transfection. The transfected Calu-3 cells were then stimulated for 6 h with 30 ng/ml human TNFα (BD Biosciences, San Jose, CA) in the absence or presence of LMWLs, CA or FP at 1–100 μM in EMEM with 1 % FBS. At 6 h, the cells were washed and harvested with 0.1 ml of the lysis reagent (Promega Corporation, Madison, WI), followed by centrifugation at 13,350 *g* for 5 min (Eppendorf). The supernatants were measured for the luciferase (Luc) activity with the 20/20n luminometer (Turner Biosystems, Sunnyvale, CA) and the total protein content by the bicinchoninic assay (BCA; Thermo Scientific, Rockford, IL). The NFκB-Luc activity of the cell lysates in each treatment group was expressed as fold-induction of the relative light unit (RLU) per mg protein, relative to the transfection control. Meanwhile, for IL-8 assessments, the non-transfected Calu-3 cells were stimulated for 6 h with 30 ng/ml TNFα in the absence or

NIH-PA Author Manuscript

NIH-PA Author Manuscript

NIH-PA Author Manuscript

presence of LMWLs, CA or FP at 0.1–100 μM in EMEM with 1 % FBS. The incubation media were analyzed for IL-8 using the enzyme-linked immunosorbent assay (ELISA; Human IL-8 ELISA MAX™ Deluxe; BioLegend, San Diego, CA). The IL-8 release in each treatment group was expressed as % IL-8 release, relative to the TNFα-stimulated control. The IC_{50} values were then determined from the concentration-dependent % IL-8 release inhibitory profile via the curve-fitting (Scientist®), as similarly described above. Finally, % IL-8 release inhibition by 10 μM CDSO3 was also determined in the Calu-3 cells stimulated with different inflammatory stimuli, 0.5 μM okadaic acid or 0.1 mM H_2O_2.

2.8. Data description and statistical analysis

The data in Figures 2–4 are expressed as mean ± standard error (SE), while the IC_{50} and HS values in Table 1 are as mean ± standard deviation (SD) of the best parameter estimates via the curve-fitting; the % inhibition values in Table 2 are also mean ± SD. Statistical analyses of the treatment group comparison employed JMP® 8 (SAS Institute, Inc., Cary, NC) or Prism® 4 (GraphPad Software, San Diego, CA). One-way analysis of variance (ANOVA) was employed to identify statistical difference between groups. Post-hoc analysis of the multiple comparison testing was then performed by the Tukey's or Dunnett's method. The p-values < 0.05 were considered as significant.

3. RESULTS

3.1. In vitro anti-elastase activities of the cinnamic acid-based LMWLs

Figure 2 shows the in vitro elastase inhibitory activities of CA and/or its unsulfated or sulfated LMWLs, CD and CDSO3, respectively, in the chromogenic substrate and insoluble elastin hydrolysis assays. The IC_{50} and HS values in the HNE hydrolysis derived through the curve-fitting are summarized in Table 1 including those for the other two sulfated LMWLs of ferulic and sinapic acid (FDSO3 and SDSO3, respectively; their concentration-dependent inhibitory profiles are not shown). As shown in Figure 2-A, while the monomer CA failed to inhibit HNE by 100 μM, its LMWLs, CD and CDSO3 both caused concentration-dependent HNE inhibition, yielding the IC_{50} values of 2.82±0.20 and 0.43±0.04 μM, respectively (Table 1). This demonstrated that oligomerizaion produced the anti-HNE activity, which was further greatly (i.e., 6.6-fold) potentiated by sulfation. Likewise, FDSO3 and SDSO3 exhibited HNE inhibition, but with slightly reduced potency (IC_{50}) of 0.55±0.04 and 0.72±0.07 μM, respectively (Table 1). As a result, CDSO3 was ranked as the most potent HNE inhibitor among the tested LWMLs. Notably, the HS values among the sulfated LMWLs (i.e., CDSO3, FDSO3 and SDSO3) were effectively comparable (1.3–1.6; Table 1), which suggested the presence of a pharmacophore in the sulfated LMWLs; the HS value for the unsulfated LMWL, CD was significantly different from its sulfated counterpart (Table 1).

Figure 2-B shows the Eadie-Hofstee plots for this HNE hydrolysis of 0.02–0.40 mM substrate in the absence or presence of 1 μM CDSO3. The K_m value was increased (0.16±0.01 → 0.37±0.07 mM), while the V_{max} value was decreased (1.21±0.07 → 1.07±0.16 $\Delta Abs_{405,10min}$), as statistically supported, which suggested the apparent mixed inhibition kinetics for CDSO3. Further, as shown in Figure 2-C, the anti-HNE activities for 0.3–1.0 μM CDSO3 increased as the preincubation time increased up to 30 min, demonstrating time-dependent inhibition; this anti-HNE activity remained essentially unaltered with longer preincubation periods (>30 min). In addition to HNE, CDSO3 also inhibited HSE with an IC_{50} value of 0.11±0.02 μM, but left PPE untouched at 100 μM (Figure 2-D). Finally, this anti-elastase activity translated into inhibition of HSE-induced degradation of insoluble elastin-congo red at 0.1–0.5 μM in a concentration-dependent fashion (Figure 2-E).

NIH-PA Author Manuscript

NIH-PA Author Manuscript

NIH-PA Author Manuscript

3.2. In vitro anti-oxidative activities of the cinnamic acid-based LMWLs

Figure 3 shows the in vitro chemical and cellular anti-oxidative activities of CA, CD or CDSO3, determined using the chemical antioxidant assay kit and H_2O_2-stimulated A549 cells, respectively. The IC_{50} and HS values in the chemical antioxidant assay derived via the curve-fitting are summarized in Table 1 including those for FDSO3 and SDSO3 (the concentration-dependent inhibitory profiles are not shown). As reported previously [17,18], the monomer CA exhibited the concentration-dependent anti-oxidative activity between 1 and 100 μM (Figure 3-A), which yielded an IC_{50} value of 16.82±1.16 μM (Table 1). This anti-oxidative activity was potentiated by oligomerization, as CD yielded a 2.7-fold lower IC_{50} value of 6.15±0.33 μM. However, unlike elastase inhibition (Figure 2-A), the sulfation of CD, as in CDSO3, resulted only in a moderate 1.7-fold increased activity (IC_{50} = 3.52±0.14 μM; Table 1). Even so, the other two sulfated LMWLs, FDSO3 and SDSO3 were less potent than CDSO3 (IC_{50} = 5.05±0.34 and 5.53±0.22 μM, respectively; Table 1), thus rating CDS as the most potent anti-oxidative LMWL. In this chemical antioxidant assay, the IC_{50} value for Trolox®, a tocopherol analogue known as an intermediate antioxidant ranked between vitamin C and E [23] was 0.29±0.03 mM. Hence, as a radical scavenging and trapping antioxidant, CDSO3 was 82.4-fold more potent than Trolox®. Notably, as shown in Table 1, the HS values among the caffeic acid-based molecules, i.e., CA, CD and CDSO3, were more closely comparable (2.9–3.7), whereas those across the sulfated LMWLs (CDSO3, FDSO3 and SDSO3) were clearly different (1.1–3.7). It was likely therefore that, in radical scavenging and trapping anti-oxidative activity, the monomeric unit is more important as a pharmacophore than the oligomer scaffolds, which was unlike the HNE inhibition (Table 1). Accordingly, in the cell system, 10 μM CDSO3 was capable of protecting the A549 cells by 70.1±15.2 % from H_2O_2-induced decrease in the rGSH level, i.e., the cellular oxidative stress, as shown in Figure 3-B. No appreciable protection was seen at 1 μM, suggesting its concentration-dependent effect.

3.3. In vitro anti-inflammatory activities of the cinnamic acid-based LMWLs

Figure 4 shows the in vitro cellular anti-inflammatory activities of LMWLs, CA and FP, determined with the TNFα-induced NFκB-Luc activity and IL-8 release in the transfected and non-transfected Calu-3 cell systems, respectively. The IC_{50} values for the TNFα-induced NFκB-Luc activities estimated from Figure 4-A are summarized in Table 1. Like the anti-HNE activity (Figure 2-A), the monomer CA had no appreciable *trans*-repression to the TNFα-induced, 1.9-fold increased NFκB-Luc activity at 100 μM, as shown in Figure 4-A. In contrast, the unsulfated and sulfated LMWLs, CDSO3, CD and FDSO3 all caused significant *trans*-repression to this inflammatory response at 10–50 μM (Figure 4-A). Unlike CDSO3, however, neither CD nor FDSO3 enabled near complete *trans*-repression at 50 μM, thereby suggesting that CDSO3 was again most potent with an IC_{50} value of ~10 μM (Table 1). Meanwhile, in this system, FP enabled similarly complete NFκB *trans*-repression at a lower 5 μM (Figure 4-A). Thus, the anti-inflammatory activity of CDSO3 was rated not as potent as that of FP, one of the most potent inhaled corticosteroids used in asthma and COPD [24]. Likewise, as shown in Figure 4-B, it was again CDSO3 that most potently inhibited the TNFα-induced IL-8 release among the tested LWMLs, given its greatest 83.7±4.6 % inhibition among the tested oligomers, when compared at 10 μM. Moreover, the inhibitory activity of IL-8 release for CDSO3 was again ranked less potent than that for FP, as FP enabled greater 94.7±2.7 % inhibition at the lower 5 μM (Figure 4-B). Figure 4-C shows the concentration-dependent inhibitory profile of this IL-8 release for CDSO3, which derived the IC_{50} value of 5.02±1.29 μM. Finally, Table 2 shows % inhibition of IL-8 release at 10 μM CDSO3 in the Calu-3 cells stimulated with different inflammatory stimuli including 0.5 μM okadaic acid and 0.1 mM H_2O_2. Despite their different initial signal transduction pathways for IL-8 release [10,25], CDSO3 equally inhibited the IL-8 release by 65.2±8.4 and 75.2±5.9 %, respectively.

NIH-PA Author Manuscript

NIH-PA Author Manuscript

NIH-PA Author Manuscript

4. DISCUSSION

We have discovered in this study that the 4-hydroxycinnamic acid-based LMWLs (Figure 1), regardless of whether they were sulfated or not, possessed potent triple inhibitory activities against elastase, oxidation and inflammation in vitro. However, as summarized in Table 1, their molar inhibitory potencies differed, depending on the monomer unit structure, oligomer scaffold and absence or presence of sulfation. As a result, among the tested LMWLs, the sulfated caffeic acid-based LMWL, CDSO3 was identified as the most potent triple inhibitor, yielding the IC_{50} values of 0.43, 3.52 and 5–10 μM, respectively (Figures 2–4; Table 1). This triple-action discovery is novel. In fact, CDSO3 appears to be the first molecule possessing high inhibitory potency against all three activities of elastolysis, oxidation and inflammation that play critical roles in emphysema and COPD [3,7,8]. Curcumin and resveratrol have been identified as dual inhibitors of oxidation and inflammation, but do not display anti-elastase activity [10–12]. New coumarinic derivatives have been shown to be anti-oxidative and anti-elastase, the latter enabling inhibition of elastase-induced inflammation, yet in a less potent fashion ($IC_{50} \geq \sim 25$ μM) [13].

The anti-HNE activities of LMWLs appeared to result from the lignin-like oligomer scaffolds rather than the monomer unit structures, which was further greatly potentiated by sulfation, e.g., 6.6-fold for CDSO3 (Figure 2-a; Table 1). This was also observed to be the case for their factor Xa and thrombin inhibition, where sulfation caused 3–10 fold greater potencies for these LMWLs [14,15]. Hence, the sulfated LMWLs are most important as a pharmacophore, as also supported by the comparable HS values (Table 1) representing like enzyme-inhibitor binding stoichiometry and cooeperativity. Accordingly, the potency differences among the sulfated LMWLs were relatively small, yet CDSO3 was ranked as the most potent HNE inhibitor (IC_{50} = 0.43 μM; Table 1). The mixed-kinetics and time dependence of this anti-HNE activity of CDSO3 (Figures 2-B and -C) generally endorsed allosteric disruption and tight or irreversible covalent binding as its inhibitory mechanism. This has also been suggested for its factor Xa and thrombin inhibition [14,15], presumably as anti-serine protease actions. Even so, this mode of inhibition should be unique, provided that most of synthetic elastase inhibitors are orthosteric, designed to directly and selectively inhibit certain catalytic domains of elastases [26,27]. In addition, as has been proven with many successful therapeutic drugs, time-dependent inhibition is also appealing for LMWLs, as it likely enables slow dissociation of the enzyme-LMWL complex (i.e., longer inhibitory activities), less affected by the substrate concentration and physiological mechanism for LMWL removal. Meanwhile, the increased anti-HNE activity by sulfation has been reported for other sulfated polysaccharides, such as heparin, chondroitin sulfates, dextran sulfates [28–31]. This was attributed to increased negative charge ($-OSO_3^-$) densities favorable for binding to positively charged HNE (PI ≈ 10) at a physiological pH [28–31]. In line with this electrostatic interaction attribute, CDSO3, again like heparin [31], exhibited more potent inhibition to more positively charged HSE (PI = 11; IC_{50} = 0.11 μM), while failing to inhibit weakly charged PPE (PI = 8–8.5; Figure 2-D).

Many synthetic HNE inhibitors have been discovered to date, which are predominantly small molecular weight (≤500 Da) molecules [26,27]. They are broadly classified into two types, acyl-enzyme inhibitors and transition-state inhibitors, and generally more potent and selective than CDSO3. However, these inhibitors have rarely succeeded presumably because of their single-mechanism inhibition that apparently cannot address the multi-faced pathogenesis of emphysema and COPD. In contrast, as a HNE inhibitor, CDSO3 displays some similarities to one of the polysaccharides, heparin. Both molecules are non-peptidic, sulfated macromolecule anticoagulants that also potently inhibit HNE (Figure 2; Table 1) [30,31]. Nevertheless, CDSO3 is structurally and mechanistically unlike heparin [14–16]. Compared to heparin, CDSO3 is based on the hydrophobic lignin-like scaffold, smaller in

NIH-PA Author Manuscript

NIH-PA Author Manuscript

NIH-PA Author Manuscript

molecular weight (3.3 kDa, compared to 12–15 kDa for heparin), and less anionic (0.8–0.9 sulfates and carboxylates per monomer, compared to 1.8 for heparin) [14–16]. In HNE inhibition, heparin acts as a noncompetitive or competitive inhibitor that requires at least 12–14 saccharides for the activity [30,31]; CDSO3 was a mixed-kinetics inhibitor (Figure 2-B) with fewer 5–13 CA units oligomerization. Collectively, therefore, CDSO3 is a distinctly new class of potent non-peptidic macromolecular HNE inhibitor that was also shown to functionally anti-elastolytic at near its IC_{50} value (Figure 2-E).

Unlike the anti-HNE activity, the anti-oxidative activities of LMWLs appeared to originate from the monomer unit activities, yet be still potentiated by oligomerization and sulfation (Figure 3-A; Table 1). The monomers, i.e., 4-hydroxycinnamic acids, caffeic, ferulic and sinapic acids, had been all shown to be radical scavenging and trapping natural phenols, and the rank-order of their anti-oxidative potencies (caffeic > ferulic > sinapic acids) [17,18] apparently led to that for the sulfated LMWLs (CDSO3 > FDSO3 > SDSO3; Table 1). As a result, despite oligomerization or sulfation, the HS values were closely comparable within the caffeic acid-based molecules (CA, CD and CDSO3), while differing among LMWLs from different monomers (Table 1), suggesting that the anti-oxidative potency and cooperativity were primarily monomer-dependent. Thus, the mechanism for this anti-oxidation of LMWLs is likely due to hydrogen donation and aromatic hydroxylation, as suggested for the monomers [17,18], even if oligomerization of 5–13 CA units resulted in only a 2.7-fold increase of the potency in the case of the caffeic acid-based LMWL (i.e., CD; Figure 3-A; Table 1). Meanwhile, the sulfation caused moderate 1.7-fold potentiation of the anti-oxidative activity (Figure 3-A; Table 1). This can be attributed to the addition of electron-withdrawing groups by sulfation causing weaker dissociation energy of O-H bonds in LMWLs, as have been suggested for other sulfated polysaccharides in the anti-oxidative activities [32,33]. As an antioxidant, CDSO3 was more potent (4.8-fold) than the monomer CA (Table 1) as well as anti-oxidative vitamin C and E or Trolox®. In addition, CDSO3 appeared to be also more potent than notable small molecule antioxidants such as resveratrol and curcumin [34,35]. In similar in vitro ABTS-based antioxidant activity assays, resveratrol was reported to be only 2.5-fold more potent than CA, while curcumin was 2.4-fold more potent than Trolox® [34,35]. In comparison, in this present study, CDSO3 was shown to be 4.8-fold more potent than CA and 82.4-fold more potent than Trolox® (Table 1). Hence, as resveratrol and curcumin have recently demonstrated their therapeutic effects in vivo [36,37], this greater anti-oxidative potency alongside functional cellular oxidative inhibition (Figure 3-B) should provide strong promise for CDSO3 to uniquely exhibit its anti-oxidative effect in cells and tissues in vivo.

As an anti-inflammatory molecule, CDSO3 was once again rated most potent among the tested LMWLs in the NFκB repression and IL-8 release inhibition with the IC_{50} values of 5–10 μM (Figure 4; Table 1). These anti-inflammatory activities were assessed in the lung epithelial cells following stimulation with TNFα, one of the “fast-responding” proinflammatory cytokines primarily from alveolar macrophages during emphysematous inflammation [3,6–8]. In epithelial cells, this TNFα has been shown to activate and translocate NFκB into the nucleus, from which several inflammatory cytokines are released, including IL-8 [10,38]. Nevertheless, in the absence of neutrophils and macrophages, this cascade generally does not involve elastases, such that the anti-inflammatory activities of LMWLs (Figure 4) unlikely resulted from their anti-elastase activities. Meanwhile, the antioxidant CA failed to be anti-inflammatory in this TNFα-induced cell system (Figure 4), presumably due to its lack of flavonoid structure [19,20]. This in turn suggested that the anti-inflammatory activities of LMWLs (Figure 4) were also unlikely the results of their inhibition of TNFα-induced oxidative stress [39,40]. Even so, the mechanism for this anti-inflammation is not fully certain at present. CDSO3 could act on TNFα and/or TNFα receptor outside the cells, quenching to trigger the subsequent inflammatory cascades. This

NIH-PA Author Manuscript

NIH-PA Author Manuscript

NIH-PA Author Manuscript

was unlikely the case, however, as CDSO3 also inhibited IL-8 release induced by other stimuli, okadaic acid and H_2O_2 (Table 2) that chemically and mechanistically differ from TNFα with respect to initial signal transduction pathways for NFκB activation and IL-8 release [10,25]. Alternatively, CDSO3 could directly act on inflammatory cascades after entering the cells like heparin [41,42] and some flavonoid molecules [10,19,43]. Despite a hydrophilic 12–15 kDa polysaccharide, heparin has been shown to inhibit inflammatory transcription factors including NFκB upon endocytosis into the cells [41,42]. Structurally as flavonoid molecules, a phenethyl ester of CA, resveratrol and curcumin have all been shown to inhibit TNFα-induced NFκB activation via intracellular suppression of inhibitory κB degradation, phosphorylation and NFκB interaction with DNA [10,19,43]. While this mechanistic clarification especially on a cellular and molecular level is of interest, CDSO3, with the IC_{50} values of 5–10 μM, seems to be more potent than these flavonoid molecules, given their effective anti-inflammatory concentrations at 88, 21 and 40 μM, respectively [10,19,43]. Hence, CDSO3 is uniquely but moderately anti-inflammatory, ranked between these flavonoid molecules and FP (Figure 4).

In conclusion, the sulfated and unsulfated 4-hydroxycinnamic acid-based LMWLs (Figure 1) are novel non-peptidic 3–4 kDa macromolecules that exhibit for the first time potent triple inhibitory activities in vitro against elastase, oxidation and inflammation, the three major pathogenic mechanisms known to cause emphysema. Among them, the sulfated caffeic acid-based LMWL, CDSO3 was most potent, yielding the IC_{50} values of 0.43, 3.52 and 5–10 μM, respectively (Figures 2–4; Table 1). Mechanistically, its anti-elastase activity resulted from the lignin-like oligomer scaffold, potentiated by sulfation, which endorsed allosteric and electrostatic disruption of the enzyme via tight or irreversible binding of CDSO3. In contrast, the anti-oxidative activity was potentiated and likely derived from the monomer CA activity, which was thus attributed to increased hydrogen donation and aromatic hydroxylation. Finally, the anti-inflammatory activity again resulting from oligomerization and sulfation was likely derived from its direct actions on the cellular inflammatory cascades, like heparin [41,42] and flavonoid molecules [10,19,43], while further studies are necessary for its cellular molecular clarification. Even so, these potent triple-inhibitory activities of CDSO3 should provide strong promise as a novel drug entity for therapeutic use in emphysema, particularly to attenuate its development and progression. Its non-peptidic macromolecular (3.3 kDa) nature should add further benefits on this venture, compared to small molecular weight or peptidic molecules, as longer lung retention and thus therapeutic longevities can be reasonably anticipated when local pulmonary delivery, such as inhalation, is employed [44]. Finally, by virtue of the triple-action inhibition, CDSO3 is likely effective in animal models of experimental emphysema, regardless of the mechanisms for their disease states induction. Such in vivo effects are now eagerly awaited for CDSO3 in different models of emphysema.

Acknowledgments

The authors are grateful to Norbert F. Voelkel, M.D. (VCU School of Medicine) for his valuable suggestions. This research was funded by the American Lung Association Biomedical Research Grant (MS; RG-159601-N) and the Medical College of Virginia Foundation. URD and JT received the funding from NIH (HL090586; HL099420) and the American Heart Association (EIA 0640053N) for LWML synthesis. BS acknowledges the financial support from the VCU School of Pharmacy and School of Graduate Studies Dissertation Award for her graduate studies.

ABBREVIATIONS

ABTS	2,2′-azinobis(3-ethyl-benzothiazoline-6-sulphonic acid)
ATCC	American Type Culture Collection

NIH-PA Author Manuscript

NIH-PA Author Manuscript

NIH-PA Author Manuscript

ANOVA	analysis of variance
BCA	bicinchoninic assay
βNADPH	β-nicotinamide adenine dinucleotide phosphate
CA	caffeic acid
CD	unsulfated caffeic acid-based low molecular weight lignin
CDS	sulfated caffeic acid-based low molecular weight lignin
COPD	chronic obstructive pulmonary disease
DMSO	dimethyl sulfoxide
DTNB	5,5′-dithiobis-(2-nitrobenzoic acid)
EDTA	ethylenediaminetetraacetic acid
ELISA	enzyme-linked immunosorbent assay
EMEM	Eagle's minimum essential medium
FBS	fetal bovine serum
FDS	sulfated ferulic acid-based low molecular weight lignin
FP	fluticasone propionate
GR	glutathione reductase
GSSG	glutathione disulfide
HNE	human neutrophil elastase
HS	Hill slope
HSE	human sputum elastase
IC_{50}	half-maximal (50 %) inhibitory concentration
IL-8	interleukin 8
K_m	the Michaelis constant
LMWL	low molecular weight lignin
Luc	luciferase
NFκB	nuclear factor kappa B
PPE	porcine pancreatic elastase
rGSH	reduced glutathione
RLU	relative light unit
tGSH	total glutathione
TNFα	tumor necrosis factor α
SD	standard deviation
SDS	sulfated sinapic acid-based low molecular weight lignin
SE	standard error
VCU	Virginia Commonwealth University
V_{max}	maximum rate

NIH-PA Author Manuscript

NIH-PA Author Manuscript

NIH-PA Author Manuscript

2-VP 2-vinyl pyridine

References

1. Kemp SV, Polkey MI, Shah PL. The epidemiology, etiology, clinical features, and natural history of emphysema. Thorac Surg Clin. 2009; 19:149–158. [PubMed: 19662957]
2. Filley GF. Emphysema and chronic bronchitis: clinical manifestations and their physiologic significance. Med Clin North Am. 1967; 51:283–292. [PubMed: 6017550]
3. Tuder, RM.; Voelkel, NF. Pathobiology of emphysema. In: Voelkel, NF.; MacNee, W., editors. Chronic obstructive lung diseases. Vol. 2. Ontario, Canada: BC Decker, Inc; 2008. p. 63-75.
4. Wise RA, Tashkin DP. Optimizing treatment of chronic obstructive pulmonary disease: an assessment of current therapy. Am J Med. 2007; 120:S4–S13. [PubMed: 17678942]
5. Barnes PJ, Stockley RA. COPD: current therapeutic interventions and future approaches. Eur Respir J. 2005; 25:1084–1106. [PubMed: 15929966]
6. Roche N, Marthan R, Berger P, Chambellan A, Chanez P, Aguilaniu B, Brillet PY, Burgel PR, Chaouat A, Devillier P, Escamilla R, Louis R, Mal H, Muir JF, Pérez T, Similowski T, Wallaert B, Aubier M. Beyond corticosteroids: future prospects in the management of inflammation in COPD. Eur Respir Rev. 2011; 20:175–182. [PubMed: 21881145]
7. Sabroe I, Parker LC, Calverley PM, Dower SK, Whyte MK. Pathological networking: a new approach to understanding COPD. Postgrad Med J. 2008; 84:259–264. [PubMed: 18508983]
8. Fischer BM, Pavlisko E, Voynow JA. Pathogenic triad in COPD: oxidative stress, protease-antiprotease imbalance, and inflammation. Int J Chron Obstruct Pulmon Dis. 2011; 6:413–421. [PubMed: 21857781]
9. Gardi C, Arezzini B, Martorana PA. Testing of compounds in models of pulmonary emphysema. Curr Med Chem. 2008; 115:803–808. [PubMed: 18393841]
10. Biswas SK, McClure D, Jimenez LA, Megson IL, Rahman I. Curcumin induces glutathione biosynthesis and inhibits NF-kappaB activation and interleukin-8 release in alveolar epithelial cells: mechanism of free radical scavenging activity. Antioxid Redox Signal. 2005; 7:32–41. [PubMed: 15650394]
11. Epstein J, Sanderson IR, Macdonald TT. Curcumin as a therapeutic agent: the evidence from in vitro, animal and human studies. Br J Nutr. 2010; 103:1545–1557. [PubMed: 20100380]
12. Rahman I, Biswas SK, Kirkham PA. Regulation of inflammation and redox signaling by dietary polyphenols. Biochem Pharmacol. 2006; 72:1439–1452. [PubMed: 16920072]
13. Bissonnette EY, Tremblay GM, Turmel V, Pirotte B, Reboud-Ravaux M. Coumarinic derivatives show anti-inflammatory effects on alveolar macrophages, but their anti-elastase activity is essential to reduce lung inflammation in vivo. Int Immunopharmacol. 2009; 9:49–54. [PubMed: 18840548]
14. Monien BH, Henry BL, Raghuraman A, Hindle M, Desai UR. Novel chemo-enzymatic oligomers of cinnamic acids as direct and indirect inhibitors of coagulation proteinases. Bioorg Med Chem. 2006; 14:7988–7998. [PubMed: 16914317]
15. Henry BL, Monien BH, Bock PE, Desai UR. A novel allosteric pathway of thrombin inhibition: Exosite II mediated potent inhibition of thrombin by chemo-enzymatic, sulfated dehydropolymers of 4-hydroxycinnamic acids. J Biol Chem. 2007; 282:31891–31899. [PubMed: 17804413]
16. Henry BL, Thakkar JN, Liang A, Desai UR. Sulfated, low molecular weight lignins inhibit a select group of heparin-binding serine proteases. Biochem Biophys Res Commun. 2012; 417:382–386. [PubMed: 22155248]
17. Gülçin İ. Antioxidant activity of caffeic acid (3,4-dihydroxycinnamic acid). Toxicology. 2006; 217:213–220. [PubMed: 16243424]
18. Rice-Evans CA, Miller NJ, Paganga G. Structure-antioxidant activity relationships of flavonoids and phenolic acids. Free Radic Biol Med. 1996; 20:933–956. [PubMed: 8743980]

NIH-PA Author Manuscript

NIH-PA Author Manuscript

NIH-PA Author Manuscript

19. Natarajan K, Singh S, Burke TR, Grunberger D. Caffeic acid phenethyl ester is a potent and specific inhibitor of activation of nuclear transcription factor NF-κB. Proc Natl Acad Sci. 1996; 93:9090–9095. [PubMed: 8799159]
20. Liao JC, Deng JS, Chiu CS, Hou WC, Huang SS, Shie PH, Huang GJ. Anti-inflammatory activities of cinnamomum cassia constitutes in vitro and in vivo. Evid Based Complement Alternat Med. 2012:429320. Epub 2012 Mar 27. [PubMed: 22536283]
21. Fujie K, Shinguh Y, Yamazaki A, Hatanaka H, Okamoto M, Okuhara M. Inhibition of elastase-induced acute inflammation and pulmonary emphysema in hamsters by a novel neutrophil elastase inhibitor FR901277. Inflamm Res. 1999; 48:160–167. [PubMed: 10219659]
22. Rahman I, Kode A, Biswas SK. Assay for quantitative determination of glutathione and glutathione disulfide levels using enzymatic recycling method. Nat Protoc. 2006; 1:3159–3165. [PubMed: 17406579]
23. Nenadis N, Lazaridou O, Tsimidou MZ. Use of reference compounds in antioxidant activity assessment. J Agric Food Chem. 2007; 55:5452–5460. [PubMed: 17579432]
24. Jaffuel D, Demoly P, Gougat C, Balaguer P, Mautino G, Godard P, Bousquet J, Mathieu M. Transcriptional potencies of inhaled glucocorticoids. Am J Respir Crit Care Med. 2000; 162:57–63. [PubMed: 10903220]
25. Sonoda Y, Kasahara T, Yamaguchi Y, Kuno K, Matsushima K, Mukaida N. Stimulation of interleukin-8 production by okadaic acid and vanadate in a human promyelocyte cell line, an HL-60 subline. Possible role of mitogen-activated protein kinase on the okadaic acid-induced NF-kappaB activation. J Biol Chem. 1997; 272:15366–15372. [PubMed: 9182566]
26. Reid PT, Sallenave J. Neutrophil-derived elastase and their inhibitors: potential role in the pathogenesis of lung disease. Curr Opin Investig Drugs. 2001; 2:59–67.
27. Ohbayashi H. Neutrophil elastase inhibitors as treatment for COPD. Expert Opin Investig Drugs. 2002; 11:065–980.
28. Lentini A, Ternai B, Ghosh P. Synthetic inhibitors of human leukocyte elastase Part 1—sulfated polysaccharides. Biochem Int. 1985; 10:221–232. [PubMed: 2581575]
29. Vilpi N. Inhibition of human leukocyte elastase activity by chondroitin sulfates. Chem Biol Interact. 1997; 105:157–167. [PubMed: 9291994]
30. Redini F, Tixier J, Petitou M, Choay J, Robert L, Hornebeck W. Inhibition of leukocyte elastase by heparin and its derivatives. Biochem J. 1988; 252:515–519. [PubMed: 3415672]
31. Spencer JL, Stone PJ, Nugent MA. New insights into the inhibition of human neutrophil elastase by heparin. Biochemisty. 2006; 45:9104–9120.
32. Wang J, Zhang Q, Zhang Z, Li Z. Antioxidant activity of sulfated polysaccharide fractions extracted from *Laminaria japonica*. Int J Biol Macromol. 2008; 42:127–132. [PubMed: 18023861]
33. Jin M, Lu Z, Huang M, Wang Y, Wang Y. Sulfated modification and antioxidant activity of exopolysaccahrides produced by *Enterobacter clocae* Z0260. Int J Biol Macromol. 2011; 48:607–612. [PubMed: 21300084]
34. Villaño D, Fernández-Pachón S, Troncoso AM, García-Parrilla MC. Comparison of antioxidant activity of wine phenolic compounds and metabolites in vitro. Anal Chim Acta. 2005; 538:391–398.
35. Prabhu PR, Hegde K, Shabaraya AR, Rao MNA. Scavenging potential of reactive oxygen species by tetra-hydrocurcumin. J Appl Pharm Sci. 2011; 1:114–118.
36. Suzuki M, Betsuyaku T, Ito Y, Nagai K, Odajima N, Moriyama C, Nasuhara Y, Nishimura M. Curcumin attenuates elastase- and cigarette smoke-induced pulmonary emphysema in mice. Am J Physiol Lung Cell Mol Physiol. 2009; 296:L614–L623. [PubMed: 19168576]
37. Birrell MA, McCluskie K, Wong S, Donnelly LE, Barnes PJ, Belvisi MG. Resveratrol, an extract of red wine, inhibits lipopolysaccharide induced airway neutrophilia and inflammatory mediators through an NF-κB-independent mechanism. FASEB J. 2005; 19:840–841. [PubMed: 15734790]
38. Fielder MA, Wernke-Dollries K, Stark JM. Inhibition of TNFa-induced NF-κB activation and IL-8 release in A549 cells with the proteasome inhibitor MG-132. Am J Respir Cell Mol Biol. 1998; 19:259–268. [PubMed: 9698598]
39. Chang SW, Ohara N, Kuo G, Voelkel NF. Tumor necrosis factor-induced lung injury is not mediated by platelet-activating factor. Am J Physiol. 1989; 257:L232–L239. [PubMed: 2801951]

NIH-PA Author Manuscript

NIH-PA Author Manuscript

NIH-PA Author Manuscript

40. Janssen-Heininger YM, Macara I, Mossman BT. Cooperativity between oxidants and tumor necrosis factor in the activation of nuclear factor (NF)-kappaB: requirement of Ras/mitogen-activated protein kinases in the activation of NF-kappaB by oxidants. Am J Respir Cell Mol Biol. 1999; 20:942–952. [PubMed: 10226064]

41. Barzu T, Molho P, Tobelem G, Petitou M, Caen J. Binding and endocytosis of heparin by human endothelial cells in culture. Biochimica et Biophysica Acta. 1985; 845:196–203. [PubMed: 3995089]

42. Wang M, He J, Mei B, Ma X, Huo Z. Therapeutic effects and anti-inflammatory mechanisms of heparin on acute lung injury in rabbits. Acad Emerg Med. 2008; 15:656–663. [PubMed: 19086324]

43. Donnelly, LE.; Barnes, PJ. Administration of resveratrol to treat inflammatory respiratory disorders. US Patent. 6878751. 2005.

44. Sakagami, M.; Gumbleton, M. Targeted drug delivery through the respiratory system: molecular control on lung absorption and disposition. In: Smyth, HDC.; Hickey, AJ., editors. Controlled pulmonary drug delivery. New York, NY: Springer; 2011. p. 127-142.

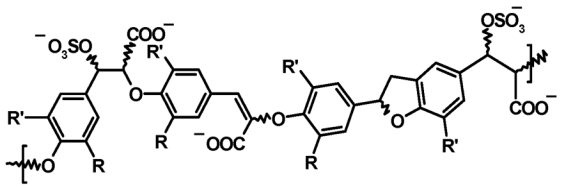

CDSO3: R = OH; R' = H
FDSO3: R = OMe; R' = H
SDSO3: R = OMe; R' = OMe

LMWL*	Range of oligomer chain length	Sulfate groups per monomer	Weight-average molecular weight [Da]
CD	5-13	NA	2,800
CDSO3	5-13	0.40	3,320
FDSO3	8-15	0.30	4,120
SDSO3	4-11	0.38	3,550

*LMWL: low molecular weight lignin. Data were taken from Henry et al [15].

Figure 1.
Unsulfated or sulfated low molecular weight lignins (LMWLs) prepared from caffeic acid (CD and CDSO3), ferulic acid (FDSO3) or sinapic acid (SDSO3) alongside their physicochemical characteristics. Chemical structures are shown as sulfated LMWLs.

NIH-PA Author Manuscript NIH-PA Author Manuscript NIH-PA Author Manuscript

NIH-PA Author Manuscript

NIH-PA Author Manuscript

NIH-PA Author Manuscript

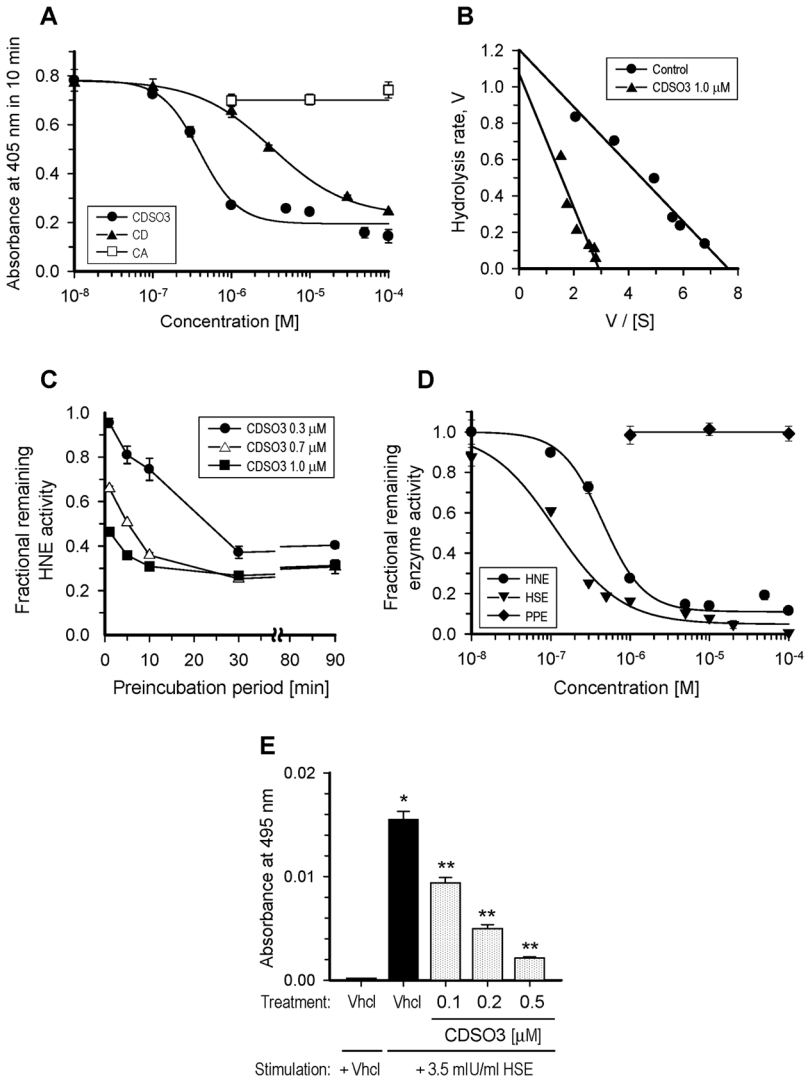

Figure 2.

In vitro elastase inhibitory activities of caffeic acid (CA) and its unsulfated or sulfated low molecular weight lignins (LMWLs; CD or CDSO3, respectively). **A.** Concentration-dependent inhibitory profiles for CA, CD and CDSO3 in the chromogenic substrate hydrolysis by 24.2 mU/ml human neutrophil elastase (HNE), monitored with the 405 nm absorbance increase in 10 min; **B.** Eddie-Hofstee plots for the HNE hydrolysis at 0.02–0.40 mM substrate in the absence or presence of 1 μM CDSO3; **C.** Effect of preincubation period on the fractional remaining HNE activities of CDSO3 at 0.3–1.0 μM. CDSO3 and HNE were preincubated for 0–90 min, prior to substrate hydrolysis; **D.** Concentration-dependent inhibitory profiles for CDSO3 in the chromogenic substrate hydrolysis by 24.2 mU/ml HNE, 3.8 mU/ml human sputum elastase (HSE) and 350 mU/ml porcine pancreatic elastase (PPE); **E.** Functional anti-elastolytic activities of CDSO3 at 0.1–0.5 μM in the 3.5 mU/ml HSE-induced elastolysis of insoluble elastin-congo red, monitored with 495 nm absorbance. Vhcl: vehicle. *p<0.05 *vs.* vehicle control; **p<0.05 *vs.* HSE-stimulated vehicle control. All data are shown as mean±SE from n=3 or 4. The solid lines are the results of the nonlinear regression curve-fitting (A and D), the linear regression (B) and the linear interpolation (C).

NIH-PA Author Manuscript

NIH-PA Author Manuscript

NIH-PA Author Manuscript

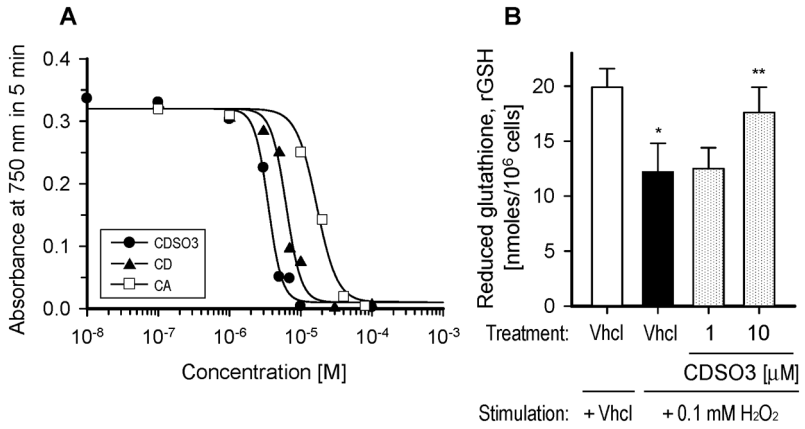

Figure 3.

In vitro chemical and cellular anti-oxidative activities of caffeic acid (CA) and its unsulfated or sulfated low molecular weight lignins (LMWLs; CD or CDSO3, respectively). **A.** Concentration-dependent anti-oxidative profiles for CA, CD and CDSO3 in the ABTS-based chemical antioxidant assay, monitored with the 750 nm absorbance increase in 5 min. The solid lines are the results of the nonlinear regression curve-fitting; **B.** Reduced glutathione (rGSH) levels in the human alveolar A549 epithelial cells stimulated for 3 h with or without 0.1 mM H_2O_2 and/or 1 or 10 μM CDSO3. Vhcl: vehicle. *$p<0.05$ *vs.* vehicle control; **$p<0.05$ *vs.* H_2O_2-stimulated vehicle control. All data are shown as mean±SE from n=3 or 4.

NIH-PA Author Manuscript
NIH-PA Author Manuscript
NIH-PA Author Manuscript

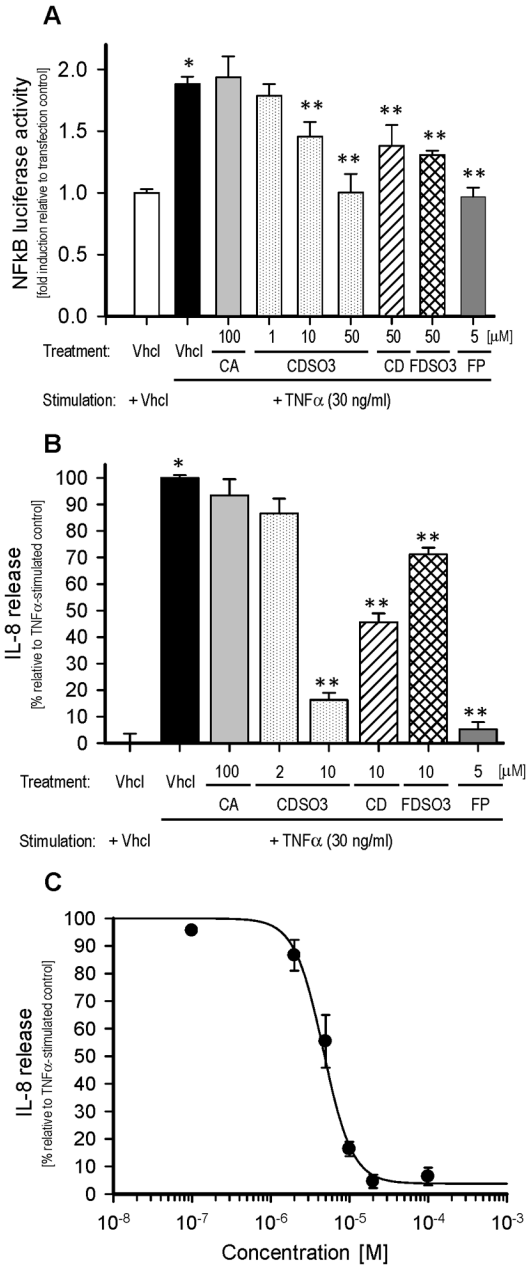

Figure 4.

In vitro anti-inflammatory activities of caffeic acid (CA), unsulfated or sulfated low molecular weight lignins (LMWLs; CDSO3, CD and FDSO3) and fluticasone propionate (FP) in the human bronchial Calu-3 epithelial cells stimulated with 30 ng/ml TNFα for 6 h. **A.** Cellular levels of the inflammatory nuclear factor kappa B (NFκB) with or without TNFα and/or 1–100 μM of the test molecules. The Calu-3 cells were transfected with pNFκB-Luc for monitoring the luciferase activities, which are expressed as folds-induction relative to transfection control; **B.** Cellular release of the inflammatory chemokine, interleukin-8 (IL-8), with or without TNFα and/or 2–100 μM of the test molecules. IL-8 release is expressed as % release relative to TNFα-stimulated vehicle control; **C.** Concentration-dependent inhibitory profile for CDSO3 to the TNFα-induced IL-8 release from the non-transfected Calu-3 cells. The solid line is the result of the nonlinear regression

curve-fitting. All data are shown as mean±SE from n=3 or 4. Vhcl: vehicle. *p<0.05 *vs.* vehicle control; **p<0.05 *vs.* TNFα-stimulated vehicle control.

NIH-PA Author Manuscript
NIH-PA Author Manuscript
NIH-PA Author Manuscript

NIH-PA Author Manuscript NIH-PA Author Manuscript NIH-PA Author Manuscript

Pulm Pharmacol Ther. Author manuscript; available in PMC 2014 April 01.

Table 1

The half-maximal inhibitory concentration (IC_{50}) and the Hill slope (HS) for caffeic acid (CA) and 4-hydroxycinnamic acid-based low molecular weight lignins (LMWLs) in the in vitro anti-elastase, anti-oxidative and anti-inflammatory activity assessments.

Molecule	Anti-elastase[1]		Anti-oxidation[2]		Anti-inflammation[3]
	IC50 [μM]	HS	IC50 [μM]	HS	IC50 [μM]
CA	NA	NA	16.82±1.16	2.9±0.5	>100
CD	2.82±0.20	1.1±0.1	6.15±0.33	3.3±0.6	~50
CDSO3	0.43±0.04	1.6±0.2	3.52±0.14	3.7±0.5	~10
FDSO3	0.55±0.04	1.3±0.1	5.05±0.34	1.4±0.2	~50
SDSO3	0.72±0.07	1.3±0.2	5.53±0.22	1.1±0.1	ND

[1] Anti-human neutrophil elastase (HNE) activity derived from the nonlinear regression curve-fitting to the *p*-nitroaniline (*p*NA) generation *vs.* concentration profiles (e.g., Figure 2-a). Values are shown as mean±SD.

[2] Anti-chemical oxidative activity derived from the nonlinear regression curve-fitting to the $ABTS^{\bullet+}$ generation *vs.* concentration profiles (e.g., Figure 3-a). Values are shown as mean±SD.

[3] Anti-inflammatory activity estimated from the TNFα-induced NFκB luciferase activity assay shown in Figure 4-a.

NA: not applicable; ND: not determined

NIH-PA Author Manuscript

NIH-PA Author Manuscript

NIH-PA Author Manuscript

Table 2

Effect of 10 μM CDSO3 on IL-8 release induced with various inflammatory stimuli in the Calu-3 cell system.

Inflammatory stimuli	% Inhibition of IL-8 release at 10 μM CDSO3
TNFα (30 ng/ml)	83.7±4.6
Okadaic acid (0.5 μM)	65.2±8.4
H_2O_2 (0.1 mM)	75.2±5.9

Data: mean±SD (n=3)